DEUTSCHES ELEKTRONEN-SYNCHROTRON DESY

DESY SR 87-08
October 1987

SOFT X-RAY GRATING EFFICIENCIES: RECIPROCITY THEOREM, BLAZE MAXIMUM AND ISOEFFICIENCY-CURVES

by

W. Jark

II. Inst. f. Experimentalphysik, Universität Hamburg

ISSN 0723-7979

NOTKESTRASSE 85 · 2 HAMBURG 52

DESY SR 87-08
October 1987

ISSN 0723-7979

SOFT X-RAY GRATING EFFICIENCIES: RECIPROCITY THEOREM, BLAZE MAXIMUM AND ISOEFFICIENCY-CURVES

Werner Jark

II. Institut für Experimentalphysik, Universität Hamburg,
Luruper Chaussee 149, 2000 Hamburg 50, Fed. Rep. of Germany
present address:
IBM Almaden Research Center, 650 Harry Road, San Jose, CA 95120-6099

ABSTRACT

In this paper data are presented that show the validity of the reciprocity theorem for diffraction by a blazed grating in the soft x-ray region. With this theorem, a simple formula for the calculation of the diffraction efficiency in blaze maximum can intuitively be derived. Calculations with this formula will be compared to experimental data for first and second order diffraction. Isoefficiency curves for these orders can also be drawn from the experimental data. These will be used to discuss the working parameters of some monochromator designs. By combining the advantages of two well-known monochromator concepts, a new design will be proposed that will allow high resolution while it can be optimized for high transmission and good suppression of higher harmonics.

presented at the 5th National Conference on Synchrotron Radiation Instrumentation, Madison WI, June 21-25, 1987 - to be published in Nucl. Instr. and Meth. A

1. INTRODUCTION

The most critical point in the design of monochromators for the soft x-ray region, where gratings will be used at grazing incidence, is the prediction of the instrumental transmission function. Recent developments in high resolution monochromators for this range lead to constant deflection designs (e.g. toroidal grating monochromators TGMs [1,2] and spherical grating monochromators SGMs [3,4]) that use only the grating between the entrance and exit slit. The efficiency for these gratings can, in principle, be calculated with sophisticated computer programs [5,6] but, unfortunately, the results cannot be parameterized. Therefore the calculations have to be repeated for every new parameter set. By choosing inappropriate grating parameters for an anticipated wavelength range without calculation, one can easily loose significantly in photon flux output from the instrument. In this paper I will present experimental data for grating efficiencies that can help in choosing working curves for monochromators in the wavelength range 1-20 nm (≃60-1200 eV). The goal of this discussion is always an optimization of the transmission characteristics of the instrument. Here the designs will not be optimized for high resolution, however the influence of some parameters on the resolution will be briefly examined.

2. THEORY

For the calculation of grating efficiencies in the soft x-ray region, the differential method [5] of the exact electromagnetic theory [7] has been shown to be successful. A comparison of the experimental data for the grating under investigation with this theory has already been described elsewhere [6]. Here I only want to deal with some special situations and present some simple formulas that allow one to calculate the efficiency without the need for really sophisticated software. Thus, only the ideas necessary to understand the derivation of these formulas will be presented. Fig 1 shows the parameters that will be used here. ϕ is the angle of grazing incidence and ψ the diffraction angle. The configuration (a) will be called the standard or nonvignetting configuration, while (b) is the reversed orientation. In the case where

ψ is larger than ϕ, the orders will be counted as positive. The second order of half the wavelength is diffracted in the same direction as the nominal wavelength and thus this light is very often referred to as second order. In order to distinguish it more clearly from the second diffraction order of the nominal wavelength it will here be called second harmonic.

The first aspect deals with the reciprocity theorem, that has not been widely recognized for diffraction grating applications in the soft x-ray region. It means that detector and source can be exchanged in a measuring device and the detected efficiency will remain the same. Maystre and McPhedran [8] have shown theoretically that, independent of groove profile and coating of the grating, this theorem is generally valid. Fig 1 illustrates this situation. Recently the validity of this theorem for the scattered light from plane mirrors was under discussion [9]. The most successful efficiency calculation procedures at present, the integral method and the differential method of the exact electromagnetic theory [7], both fulfill this theorem up to several digits after the decimal point [5]. The first attempts [10,11] to calculate the efficiency in the soft x-ray regime for grazing incidence with a scalar theory lead to formulas that obviously do not generally include this theorem. Lukirskii and Savinov [11] have already observed and mentioned comparable efficiencies in blaze maxima for situations where the reciprocity theorem would be applicable, but they could not satisfactorily explain this observation with the derived formulas.

Based on the reciprocity theorem, Maystre and Petit [12] derived intuitively, with geometrical arguments, the following formula for the calculation of the efficiency in the blaze maximum case. In this configuration the first order is reflected at the groove, consequently one would expect the efficiency in the nonvignetting configuration (Fig 1a) to be equal to the reflection coefficient for the groove $R(\phi^*)$, where ϕ^* is the angle of grazing incidence onto the groove facet (see Fig 6). In the reversed orientation (Fig 1b) there is obviously intensity lost in the valleys of the sawtooth profile. Thus the

nonvignetting area is proportional to $\frac{sin\phi}{sin\psi}$, so that with geometrical arguments the efficiency e_{BM} would be expected to be

$$e_{BM} = R(\phi^*)\frac{sin\phi}{sin\psi} .$$

If the reciprocity theorem is valid, the efficiencies in the two orientations of Fig 1 are identical. Then for blaze maximum they can be calculated with the formula [12]

$$e_{BM} = R(\phi^*)\min\left(\frac{sin\phi}{sin\psi}, \frac{sin\psi}{sin\phi}\right) \qquad (1),$$

where $\min\left(\frac{sin\phi}{sin\psi}, \frac{sin\psi}{sin\phi}\right)$ is always smaller than 1. This formula is in very good agreement with the exact calculations [12]. So obviously, even for the nonvignetting configuration, the efficiency in blaze maximum can be significantly smaller than the reflection coefficient.

3. EXPERIMENTAL

The data presented here deal with only one parameter set for a plane grating whose groove profile was holographically recorded and ion-etched into a quartz substrate (manufacturer ASTRON). These parameters, i.e. 1200 lines/mm, blaze angle 1.5° and gold coating, are frequently chosen and in the soft x-ray region they are usually used at grazing incidence to monochromatize the shortest wavelengths. No data will thus be presented for normal incidence where the expected efficiency can still be derived from universal efficiency curves [13]. Reported here will be efficiencies that have been measured at grazing incidence for wavelengths between 1 and 20 nm. The data were collected in the classical orientation, i.e. with the grooves perpendicular to the plane of incidence, and with the nearly linearly polarized electric vector E perpendicular to this plane. This situation is usually referred to as s-polarization or TE mode and it is the orientation always used for grating monochromators at synchrotron radiation sources.

This investigation was carried out at beamline G1 at HASYLAB which is supplied with synchrotron radiation by the storage ring DORIS [14]. The instruments, i.e. the UHV-reflectometer [15] and the monochromator BUMBLE BEE [16,17], are described in great detail elsewhere. The experimental details are given in ref. [6]. For the present data it shall only be mentioned that most of the experiments were performed by rotating a detector around the grating set to a fixed angle of grazing incidence. The detector can also follow a specific diffraction order in a scan versus the angle of grazing incidence. The size of the detector aperture was chosen so that neither beam broadening after the diffraction nor overlapping of different orders have to be deconvoluted from the measured data. Second order content and stray light in the monochromatized light make up at most 2% of the signal [17]. Usually the data could be corrected for the stray light content, so systematic errors are smaller than 2%. Hence error bars would usually have to be smaller than the plotted points and thus, for a clearer representation, they are always omitted.

3.1. THE RECIPROCITY THEOREM

The validity of this theorem for a specific situation, the blaze maximum condition at $\lambda = 10$ nm, is demonstrated in Fig 2, where the intensity distribution after diffraction at the grating in the two orientations of Fig 1 is shown. The data are plotted versus the deflection angle $(\phi + \psi)$ at the grating, so we find the two corresponding diffraction orders - i.e. the first positive in the standard configuration and the first negative in the reversed one - at the same angular position. An efficiency of approximately 31.2% was measured in both orientations.

A systematic investigation of this theorem has not been presented until now, hence in Fig 3 the validity of this theorem is shown more generally for the diffraction efficiencies into the second orders at $\lambda = 10$ nm. The decisive parameter is the deflection angle $(\phi + \psi)$ at the grating, so all values measured for both orientations are plotted versus this parameter. We must always compare a positive order with a negative one. The fact that corresponding data can be represented very well by a single curve supports the validity of the reciprocity theorem. Comparably good

agreement was found for all investigated wavelengths, without any exception, for up to the third orders.

It is also interesting to test this theorem with the zeroth order. These data measured in both orientations as a function of the angle of grazing incidence ϕ are presented in Fig 4 for 2 wavelengths. Despite the fact that the blazed grating profile is not symmetrical with respect to the normal onto the surface, the efficiencies agree very well with each other. Obviously the reciprocity theorem is valid for the soft x-ray region for the parameter investigated here. Hence, starting at this point, all the other data will only be given for the nonvignetting configuration that is usually chosen in blazed grating mounts. Simple geometrical calculations allow conversion of the angles to the other orientation.

3.2 BLAZE MAXIMUM

An important configuration for blazed gratings is the blaze maximum orientation where the first diffraction order, and consequently all higher harmonics, are reflected at the grooves. The monochromators described by Dietrich and Kunz [18], Hunter et al [19] and Jark et al [16] are especially designed to maintain this blaze maximum condition while scanning the wavelength.

The first order efficiency data for this condition in the standard orientation are presented in Fig 5. In order to test the applicability of formula (1), these data were divided by the reflectivity $R(\phi^{*})$ calculated for the angle of grazing incidence ϕ^{*} onto the grooves. Fresnel equations were used in combination with the atomic scattering factors tabulated by Henke et al [20]. After a further division by the geometrical factor $\min\left(\frac{\sin\phi}{\sin\psi}, \frac{\sin\psi}{\sin\phi}\right)$, the results are plotted in Fig 6. If formula (1) is valid, all data should not significantly deviate from unity. This is obviously true for the theoretical results that were obtained from calculations with the differential method [6,21]. The experimental data lead to smaller ratios. For 3 nm $\leq \lambda \leq$ 10 nm, approximately 2/3 of the estimation is reached. Starting at wavelength 2.5 nm, where just half of each groove is illuminated, the ratio drops. Departure from the ideal shape for the top edge of the grooves may be responsible for this. This contributes increasingly to the illuminated area and will thus reduce the efficiency compared to the calculations. So formula (1) gives a satisfactory estimate for the +1. order efficiency of the investigated grating only for $\lambda \geq 3$ nm. For the second harmonic (or the second order) the calculations once more support the applicability of the simplified formula (1). On the other hand, the experimental data can no longer consistently be calculated by slightly modifying this formula.

For most of the experiments in the soft x-ray region, a significant suppression of the higher harmonics in the monochromatized light is anticipated. It is thus interesting to note here that the efficiency of the second order is much worse than expected, leading to much better suppression of the second harmonic than theoretically expected. In order to predict the photon flux behind their monochromators, Hunter et al [19] and Jark et al [16] have used a formula for blaze maximum $e_{BM} = CR(\phi^*)$, with C = 0.1 [16] and C = 0.4 [19] that does not take into account the geometrical factor of formula (1). The results here show that calculations with this formula will not lead to reliable data for the expected transmission of these instruments and especially not for the suppression of the higher harmonics.

3.3 ISOEFFICIENCY CURVES

In order to prepare the measured data so that they are more useful for monochromator design, they will not be presented in the usual form of angular dependent efficiencies at constant wavelength, but they will be drawn into $\phi = f(\lambda)$ diagrams. In Fig 7 the curves for the efficiency maximum and for the half maximum positions of the angle dependent efficiency profiles are shown following the "grating efficiency map" introduced by Petersen [22]. Curve b indicates the blaze maximum

condition for the investigated grating, making it obvious that the maximum efficiency is not necessarily found close to blaze maximum.

Regarding the efficiency, the present data allow us to go into more detail, so Fig 8 shows the isoefficiency curves for the first order and the second harmonic. In order to locate areas where this grating will not efficiently suppress the second harmonic, both plots can be directly compared with each other. It is immediately obvious that the curves for the first order maximum and for the second harmonic maximum are not far apart. The data are too incomplete to derive curves with constant suppression power for the second harmonic, however the curves for the second harmonic can be normalized with the maximum efficiency for the first order. Those data are given in Fig 9. Comparing this diagram with Fig 7 shows that the 10% lines lie mostly well within the FWHM of the angular dependent first order efficiency curves, i.e. in worst case they are actually the 20% lines for second harmonic suppression. In addition to these curves, bars of different thickness indicate regions where the efficiency of the second harmonic can reach values of 30% and 50% of the first order maximum efficiency. Consequently the enclosed areas should be avoided in monochromator designs that use a similar grating and no other component to suppress the second harmonic. While this may lead to significant flux reductions in some intervals, this grating performs particularly well around $\lambda = 10$ nm, where additionally the efficiency maximum is found in Fig 8. The small absorption coefficient of gold near 10 nm is responsible for this, it leads to comparably high reflectivities in the case of mirrors and consequently here to high efficiencies.

What conclusions can we draw from Fig 7 to Fig 9? Let us assume that the "grating efficiency map" in Fig 7 is also a good description for groove densities other than 1200 lines/mm. Fig 8 and Fig 9 are too specific, so they are reliable only for 1200 lines/mm but they may at least show the tendencies for other gratings too. Ideally, a monochromator design should allow every point in the angle-wavelength diagram of

Fig 7 to be reached, then, dependent on the experiment, either flux or second harmonic suppression can be optimized for every wavelength. This is fulfilled in the plane grating monochromators described by Dietrich and Kunz [18], Petersen and Baumgärtel [23], Hunter et al [19], and Jark et al [16]. In order to keep the directions of the incident and the exit beam fixed, these monochromators always need at least 2 optical components that have to be scanned together. The blaze maximum curve b in Fig 7, for example, is also a working curve for one of these monochromators [16,17] for simultaneous rotations of the grating and a premirror. It leads to high flux while the second harmonics are well suppressed for $\lambda \geq 6$ nm.

All those designs that use a fixed deflection angle θ at the grating and scan the wavelength by rotating just this grating, result in working curves that intersect the angle axis at $\frac{\theta}{2}$ and the wavelength axis at the horizon wavelength $\lambda_h = 2d\sin(\frac{\theta}{2})$, where d is the grating constant. The curves a in Fig 7 represent this kind of working curve for a TGM (toroidal grating monochromator) [2] with $\theta = 8°$. It is interesting to note that the photon flux curves, especially for 1200 lines/mm and 1800 lines/mm gratings [2], agree well with Fig 7. This design will thus be briefly discussed here. For this monochromator concept the slit width limited resolution for a given wavelength worsens with decreasing groove density. On the other hand, a large tuning range requires a small groove density, so that, in order to extend the tuning range to longer wavelengths, resolution has to be sacrificed. As a compromise, usually several gratings will be used with the same deflection angle. Discussing the working curves a from Fig 7 with Fig 9 makes the biggest problem with this design obvious: all 3 curves cross the area with small second harmonic suppression power.

Working curves with opposite slope published by Howells [24] for a special plane grating design seem to lead to better working data. But this design monochromatizes in the reversed orientation and can thus not be discussed with Fig 7. However, the reciprocity theorem allows source and detector (i.e. exit slit) to be exchanged in this

design, and the converted working curves are very similar to the TGM curves a in Fig 7. On the other hand, this design, as well as the FLIPPER monochromator [25], overcome the limited tuning capability by using additional components in the instrument that allow the use of different deflection angles at the grating. While in the FLIPPER several exchangeable premirrors with different deflection angles are installed in front of the grating, both instruments use focussing off-axis paraboloids behind the grating. Figure errors in this last aspherical component do not yet allow the theoretical resolution to be achieved when the complete mirror is illuminated. Small areas on the paraboloid of the FLIPPER are ideally shaped, so by reducing the acceptance of this monochromator the theoretical resolution limit can be reached with significant losses in photon flux [26].

Further examples of instruments using different deflection angles are the TGM design [2] already discussed, that is a combination of two TGM monochromators, and the LOCUST [27], where the grasshopper design [28] is modified so that 4 separate gratings can be used with different deflection angles.

In order to achieve the very small figure errors necessary for high resolution, recent developments lead to designs very similar to the TGMs but using spherical gratings [3,4], because this self-generating surface can be polished very close to the ideal shape, with figure errors of less than 1 arc second, prior to groove etching. Based on these gratings, I want to propose a design that allows high resolution while it is optimized also for high flux over a larger tuning range and can be optimized for good suppression of higher harmonics. The design idea is presented in Fig 10, it combines the order sorting premirror configuration of the FLIPPER [25] with the SGM (spherical grating monochromator) concept (it can as well be used in TGMs). In this design different deflection angles at the grating can be realized in a configuration with fixed entrance and exit direction. The additional plane mirrors that will determine the deflection angle at the grating have to be placed between the two slits. These slits have limited travel along the beam direction and in order to use a number of mirrors in conjunction with them we have to use the appropriate radii of curvature for the gratings. These radii change with the deflection angle, so this design requires as many gratings with different radii as mirrors. While the groove density usually is varied, here groove density and blaze angle - or groove depth - can be the same for all gratings (e.g. 1200 lines/mm). In addition to the figure errors of the grating, now the figure errors of the plane mirrors will also increase the size of the monochromatic image in the slit and hence reduce the resolving power. In order to keep the contribution of these additional mirrors small, they have to be very close to the exit slit. They can be installed either in front of the grating or behind it. For high resolution, the last configuration has to be chosen, while, to protect the sensitive grating surface from heat load and contamination, one would rather put them in front of the grating. The overall length of these mirrors would be comparable with the grating dimensions or even shorter. So this concept could be realized in a compact instrument, that will be easy to operate.

Furthermore, this design offers another nice feature. In case that one of the gratings is used with the "wrong" mirror leading to a deflection angle that is larger than that with the "right" mirror, the focus will still lie on the Rowland circle [29]. But now the optimal distance entrance slit - exit slit is increased compared to the "right" combination, so with the entrance slit position kept, the new monochromatic focus is farther away from the grating. If the original slit is now opened or removed, a second slit can be installed at the new focus position, and thus another experimental chamber behind the first could alternatively be supplied with monochromatic light. This would allow two different experimental stations to be permanently installed after this instrument.

4. CONCLUSION

It is shown, that for a diffraction grating in the classical orientation, the reciprocity theorem is valid in the soft x-ray region up to at least the third diffraction order. Consequently, detector and source can be exchanged and the efficiency remains unchanged. Based on the validity of this theorem a simple formula for the calculation of the efficiency in blaze maximum can intuitively be derived. This formula is in good agreement with the exact calculations, but it overestimates the efficiency of the investigated grating for $\lambda \geq 3$ nm consistently by about 35%. For shorter wavelengths, the quality of the upper edge of the sawtooth profile starts to affect the efficiency. The more a non-ideal edge contributes to the total illuminated length of the grooves, the more the efficiency is reduced compared to that estimated with the simple formula (1). By using the isoefficiency curves derived for this grating for the first and second diffraction orders, problematic working regions of some monochromator designs are pointed out. Thus, a new concept is presented that combines the SGM design with the order sorting mirrors of the FLIPPER monochromator. This instrument will allow high resolution, while it can additionally be optimized over a larger wavelength range for high flux and good higher harmonic suppression.

ACKNOWLEDGEMENT

I gratefully acknowledge many illuminating discussions with C. Kunz. Furthermore I want to thank M. Neviere for contributing the exact calculations for the blaze maximum efficiencies to this study. This work was supported by the Bundesministerium für Forschung und Technologie under contract No. 05 248 Ku and No. 05 305 AX B/5.

FIGURE CAPTIONS

Fig. 1) Angle convention for the present study:

(a) standard configuration

(b) reversed orientation.

The situation where the reciprocity theorem should be valid is shown.

Fig. 2) Intensity distribution of monochromatic light with wavelength $\lambda = 10$ nm after diffraction at the grating in blaze maximum for the two configurations shown in Fig 1. Arrows point to the orders that should fulfill the reciprocity theorem, while numbers indicate the order numbers.

Fig. 3) Grating efficiencies $e_{\pm 2}$ measured for the second orders versus the deflection angle $(\phi + \psi)$ at the grating for the two configurations of Fig 1.

Fig. 4) Grating efficiencies measured for the zeroth orders versus the angle of grazing incidence ϕ for 2 wavelengths. Small letters refer to the configurations shown in Fig 1:

(a) standard configuration and (b) reversed orientation.

Fig. 5) Grating efficiencies measured for the first positive orders in blaze maximum in the standard configuration versus wavelength: comparison of the measured values with the calculations using the differential method [5] of the exact theory.

Fig. 6) Grating efficiencies from Fig 5 divided by formula [1]: comparison between the measurements and the calculations for

(a) the first diffraction order

(b) the second diffraction order.

Fig. 7) "Grating efficiency map" according to Petersen [22] for the grating investigated: plot of the position of maximum efficiency $e_{+1,max}$ and of the two half maximum positions $\frac{max}{2}$ against wavelength. Small letters indicate

(a) working curve for a TGM monochromator [2] with 8° deflection angle and gratings with 1800 lines/mm, 1200 lines/mm and 800 lines/mm (left to right).

(b) blaze maximum curve for 1200 lines/mm and blaze angle 1.5°

Fig. 8) Isoefficiency curves for a blazed grating in the standard configuration:

left: for the first diffraction order

right: for the second harmonic i.e. the second order of half the wavelength.

Question marks indicate areas where experimental data for supporting the lines are not available.

Fig. 9) Diagram with lines of constant suppression power for the second harmonic against wavelength. The lines enclose those areas where the efficiency for the second harmonic is at least 10% of the maximum efficiency of the first order. Bars of different thickness indicate intervals where the ratio is 30% and 50%, respectively.

Fig. 10) Schematic view of a proposed modified spherical grating monochromator:

G_{1-3} : exchangeable spherical gratings with different radii of curvature and e.g. identical groove density.

M_0 : mirror configuration, that focuses the beam vertically onto the entrance slit and horizontally approximately onto the exit slit.

M_{1-3} : additional mirrors, enabling different angles of deflection to be realized at the gratings (M_2 and M_3 are removable sideways from the beam (arrows)).

S_1 : entrance slit (movable along the beam).

S_2 : exit slit (movable along the beam).

The components and distances are not drawn to scale.

REFERENCES

(1) C. T. Chen, E. W. Plummer and M. R. Howells, Nucl. Instr. and Meth. 222, 103 (1984)

(2) F. J. Himpsel, Y. Jugnet, D. E. Eastman, J. J. Donelon, D. Grimm, G. Landgren, A. Marx, J. F. Morar, C. Oden, R. A. Pollak and J. Schneir, Nucl. Instr. and Meth. 222, 107 (1984)

(3) M. C. Hettrick and J. H. Underwood, Appl. Opt. 25, 4228 (1986)

(4) H. Hogrefe, M. R. Howells and E. Hoyer, to be published in Soft X-Ray Optics and Technology, Proc. SPIE 733 (1986)

(5) M. Neviere, P. Vincent and R. Petit, Nouv. Rev. Opt. 5, 65 (1974)

(6) W. Jark and M. Neviere, Appl. Opt. 26, 943 (1987)

(7) Electromagnetic Theory of Gratings, Topics in Current Physics 22, Editor: R. Petit (Springer Verlag, Berlin 1980)

(8) D. Maystre and R. C. McPhedran, Opt. Commun. 12, 164 (1974)

(9) H. Okayama and I. Ogura, Appl. Opt. 23, 3349 (1984)
H. J. Eom, Appl. Opt. 24, 1730 (1985)
W. H. Venable, Appl. Opt. 24, 3943 (1985)

(10) G. Sprague, D. H. Tomboulian and D. E. Bedo, J. Opt. Soc. Am. 45, 756 (1955)

(11) A. P. Lukirskii and E. P. Savinov, Opt. Spectrosc. 14, 147 (1963)

(12) D. Maystre and R. Petit, Nouv. Rev. Opt. 7, 165 (1976)

(13) E. G. Loewen, M. Neviere and D. Maystre, Appl. Opt. 16, 2711 (1977)
E. G. Loewen and M. Neviere, Appl. Opt. 17, 1087 (1978)

(14) H. E. Behrend, E. E. Koch, C. Kunz and G. Mülhaupt, Nucl. Instr. and Meth. 152, 37 (1978)

(15) H. Hogrefe, D. Giesenberg, R.-P. Haelbich and C. Kunz, Nucl. Instr. and Meth. 208, 415 (1983)
H. Hogrefe, R. P. Haelbich and C. Kunz, Nucl. Instr. and Meth. A246, 198 (1986)

(16) W. Jark, R.-P. Haelbich, H. Hogrefe and C. Kunz, Nucl. Instr. and Meth. 208, 315 (1983)

(17) W. Jark and C. Kunz, Nucl. Instr. and Meth. A246, 320 (1986)

(18) H. Dietrich and C. Kunz, Rev. Sci. Instrum. 43, 434 (1972)

(19) W. R. Hunter, R. T. Williams, J. C. Rife, J. P. Kirkland and M. N. Kabler, Nucl. Instr. and Meth. 195, 141 (1982)

(20) B. L. Henke, P. Lee, T. J. Tanaka, R. L. Shimabukuro and B. K. Fujikawa, At. Dat. Nucl. Dat. Tables 27, 1 (1982)

(21) M. Neviere, University of Marseille, unpublished results 1985

(22) H. Petersen, Opt. Commun. 40, 402 (1982)

(23) H. Petersen and H. Baumgärtel, Nucl. Instr. and Meth. 172, 191 (1980)

(24) M. R. Howells, Nucl. Instr. and Meth. 177, 127 (1980)

(25) W. Eberhardt, G. Kalkoffen and C. Kunz, Nucl. Instr. and Meth. 152, 81 (1978)

(26) F. Senf and S. Cramm, University of Hamburg, private communications 1986.

(27) R. Z. Bachrach, R. D. Bringans, B. B. Pate and R. G. Carr, Insertion Devices for Synchrotron sources, Proc. SPIE 582, 251 (1985)

(28) F. C. Brown, R. Z. Bachrach and N. Lien, Nucl. Instr. and Meth. 152, 73 (1978)

(29) H. A. Rowland, Phil. Mag. 13, 469 (1882)

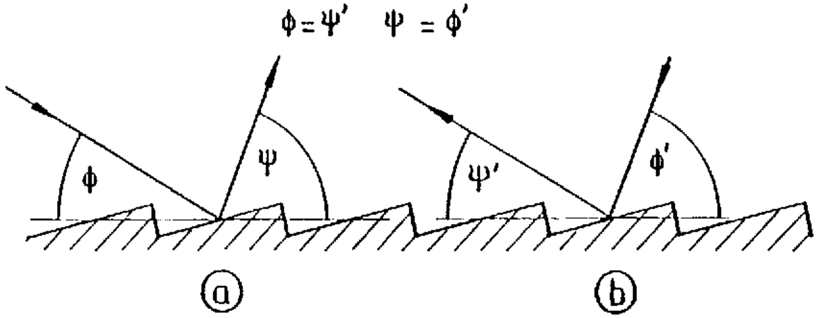

φ = ψ'   ψ = φ'
φ
ψ
ψ'
φ'
a
b

Fig 1

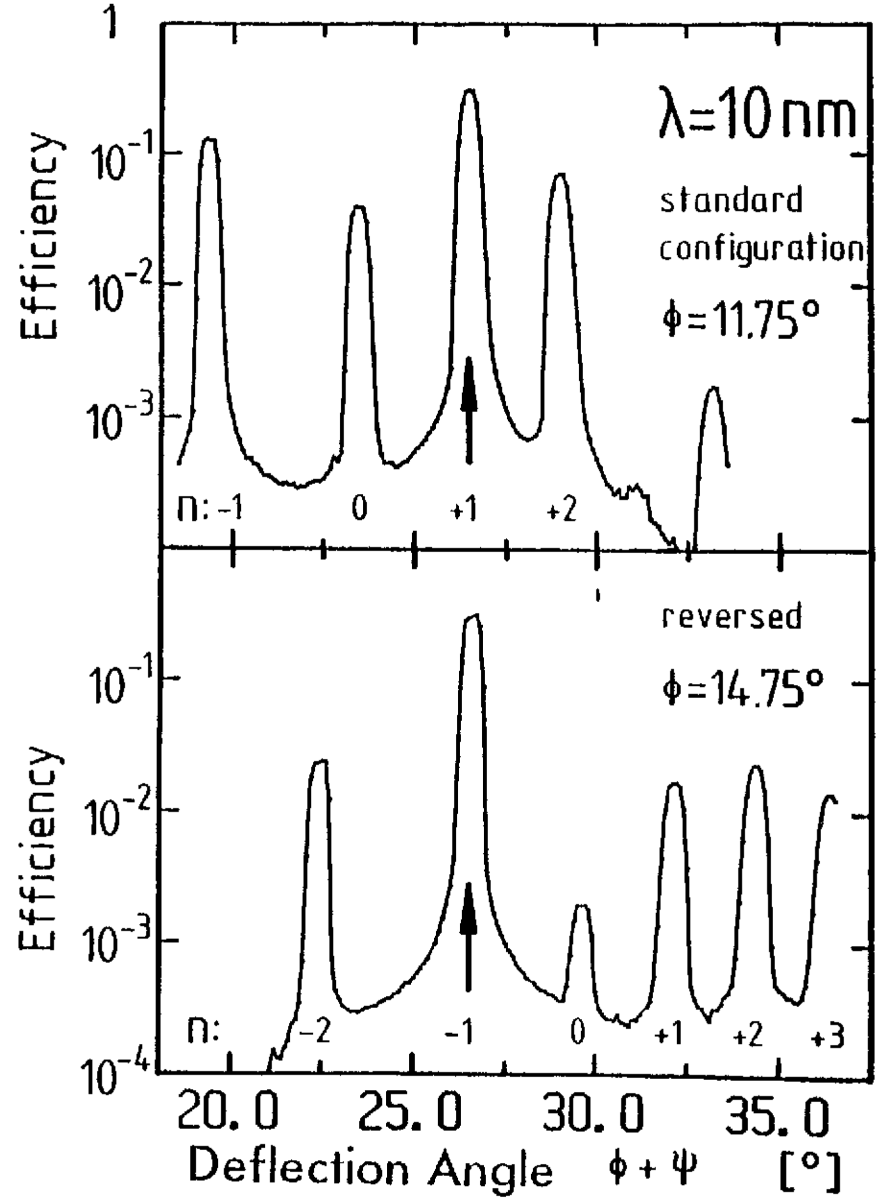

λ=10 nm
standard configuration
φ=11.75°
reversed
φ=14.75°
Efficiency
Efficiency
1
10⁻¹
10⁻²
10⁻³
10⁻⁴
n: -1
0
+1
+2
n:
-2
-1
0
+1
+2
+3
20.0
25.0
30.0
35.0
Deflection Angle φ + ψ [°]

Fig 2

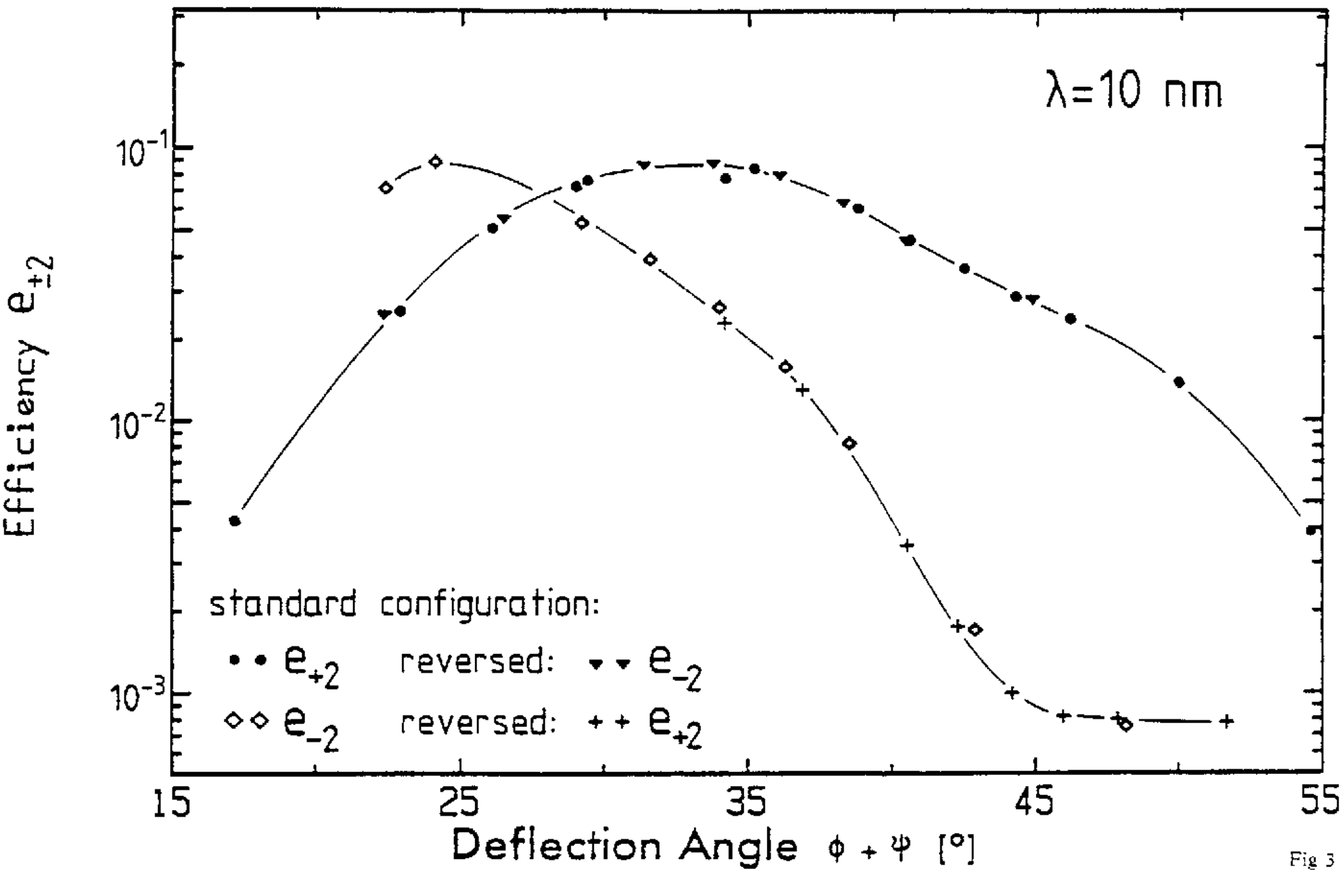

λ=10 nm
Efficiency $e_{\pm 2}$
10^{-1}
10^{-2}
10^{-3}
standard configuration:
e_{+2} reversed: e_{-2}
e_{-2} reversed: e_{+2}
15
25
35
45
55
Deflection Angle $\phi + \psi$ [°]

Fig 3

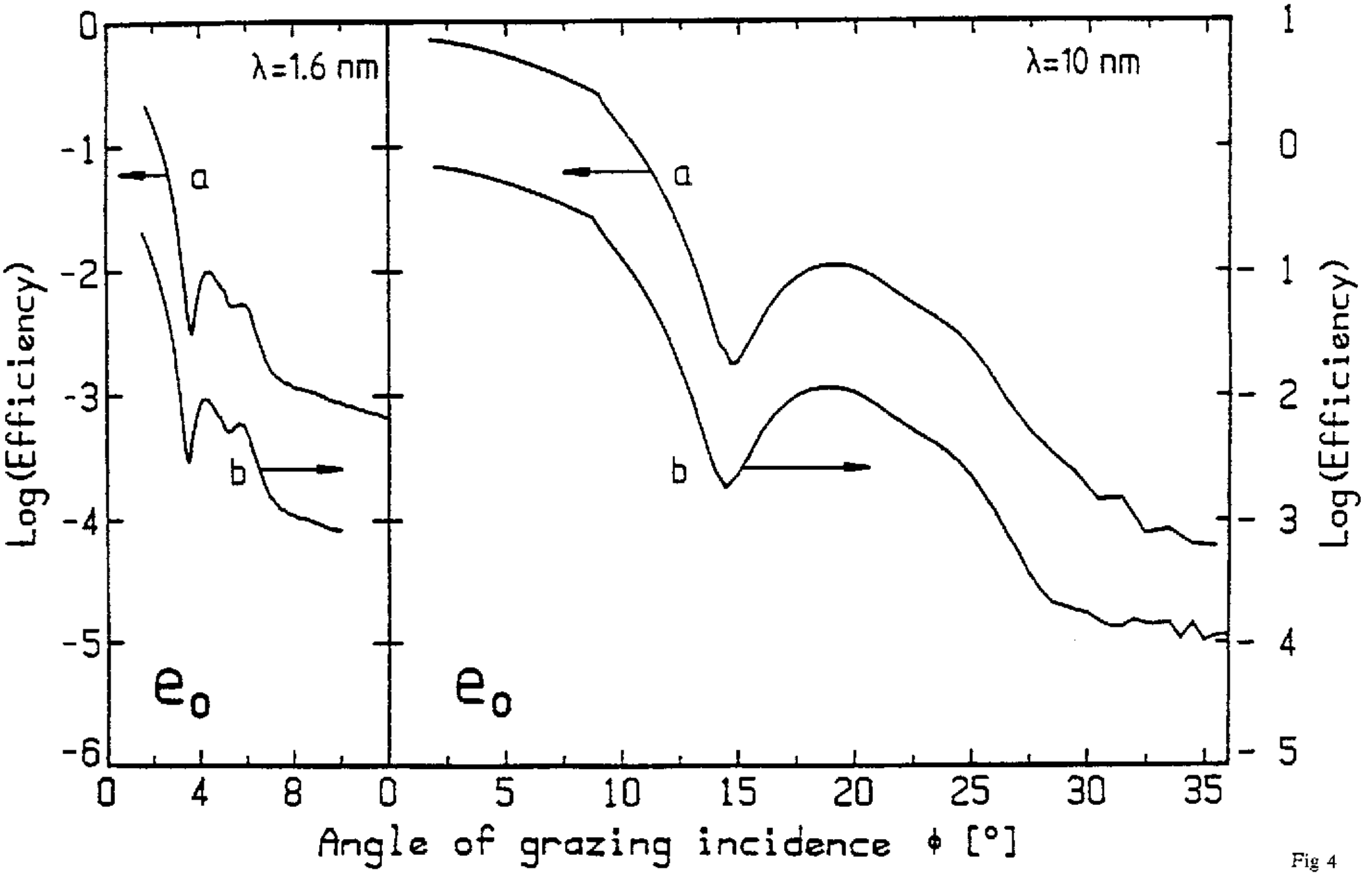

λ=1.6 nm
λ=10 nm
a
b
e_0
e_0
Log(Efficiency)
Log(Efficiency)
Angle of grazing incidence ϕ [°]

Fig 4

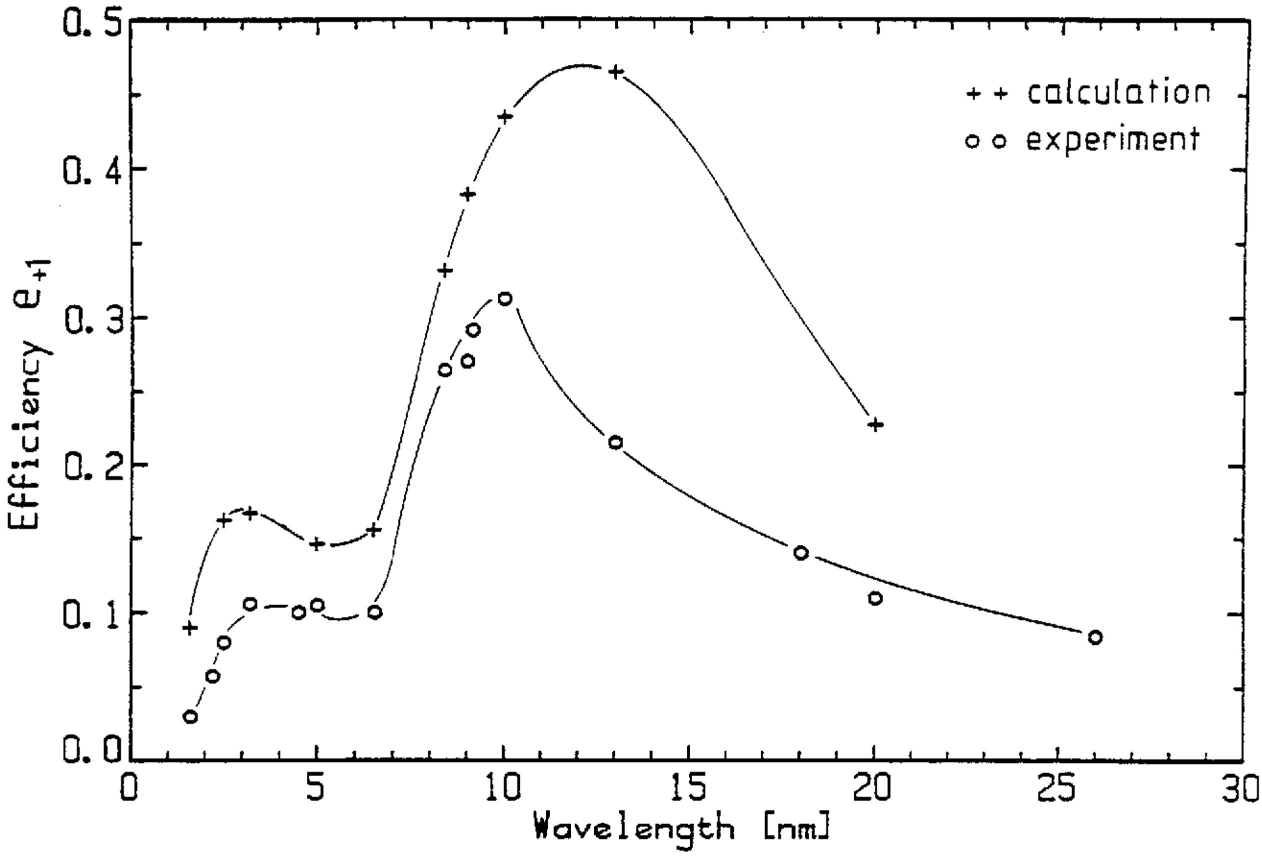

0.5
0.4
0.3
0.2
0.1
0.0
Efficiency e_{+1}
0
5
10
15
20
25
30
Wavelength [nm]
+ + calculation
o o experiment

Fig 5

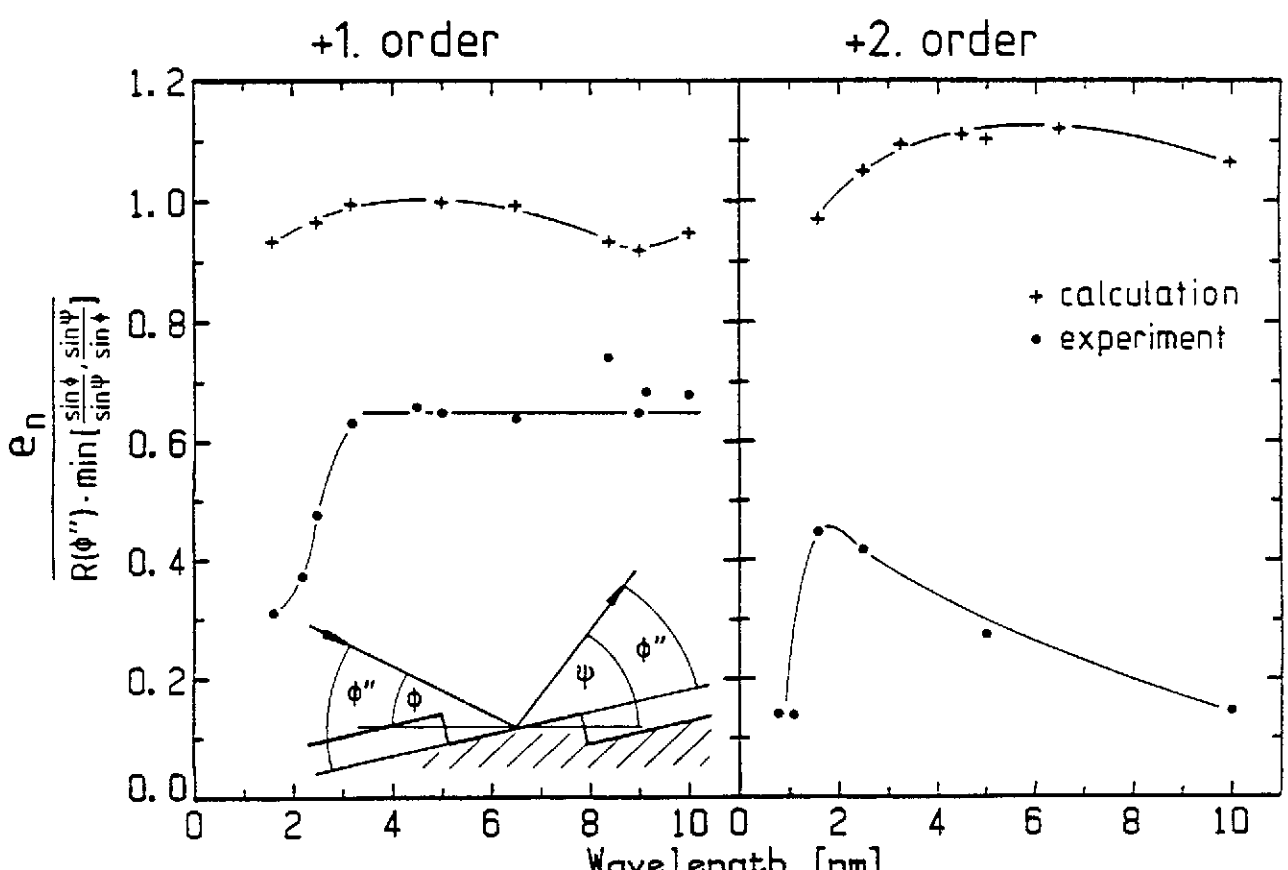

+1. order
+2. order
1.2
1.0
0.8
0.6
0.4
0.2
0.0
$\frac{e_n}{R(\phi'')\cdot \min[\frac{\sin\phi}{\sin\psi},\frac{\sin\psi}{\sin\phi}]}$
0
2
4
6
8
10
Wavelength [nm]
+ calculation
• experiment
φ''
φ
ψ
φ''

Fig 6

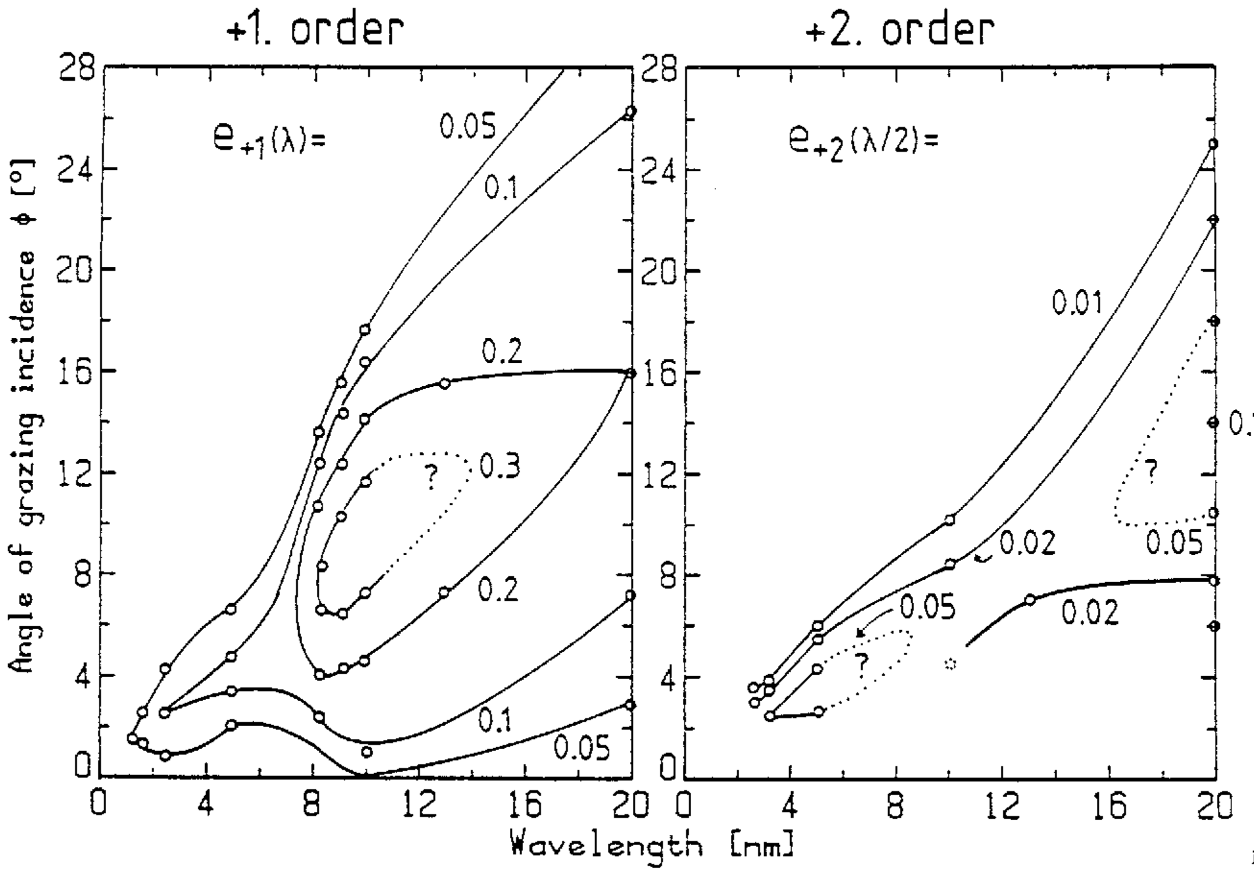
+1. order
+2. order
Angle of grazing incidence φ [°]
$e_{+1}(\lambda)=$
$e_{+2}(\lambda/2)=$
0.05
0.1
0.2
0.3
0.01
0.02
?
Wavelength [nm]

Fig 8

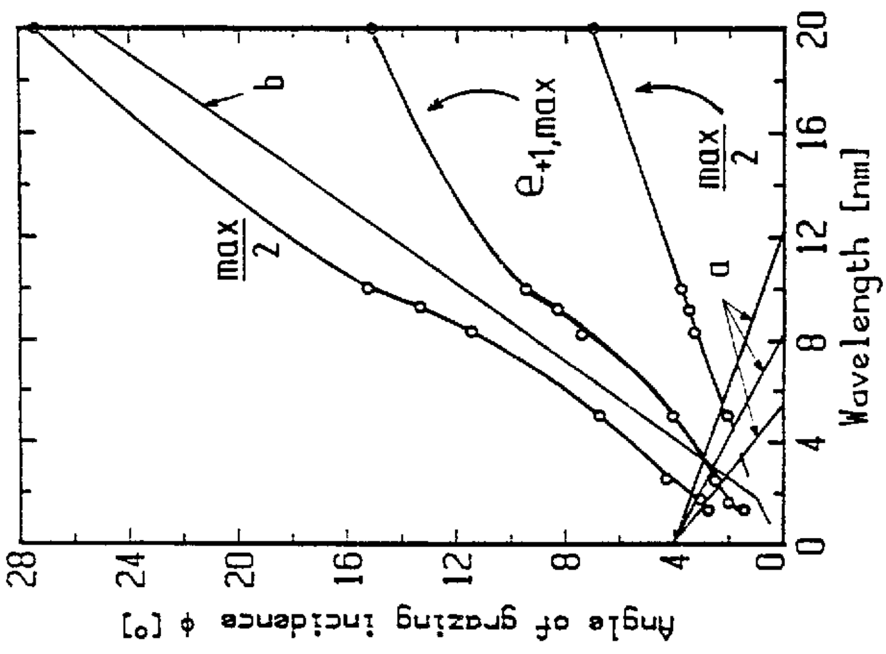
Angle of grazing incidence φ [o]
Wavelength [nm]
$e_{+1,max}$
max/2
a
b

Fig 7

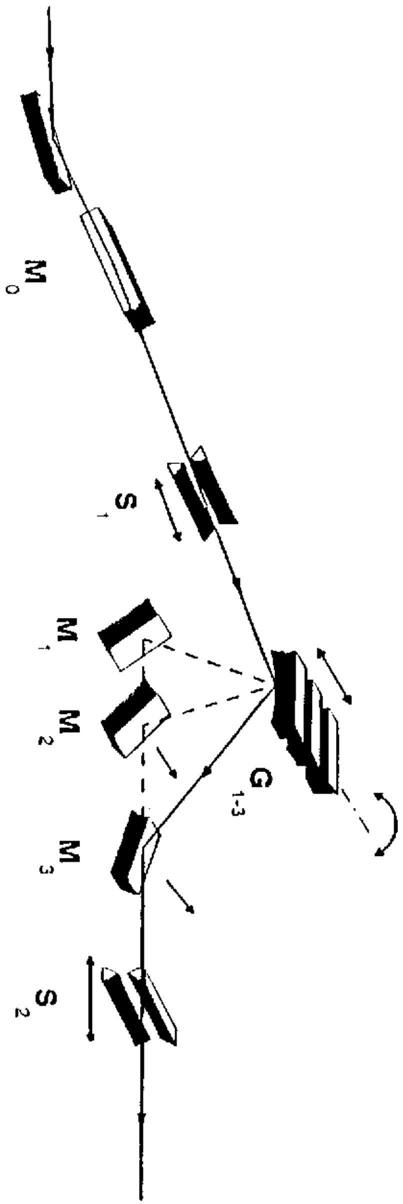
M0
S1
M1
M2
M3
G1-3
S2

FIG. 10

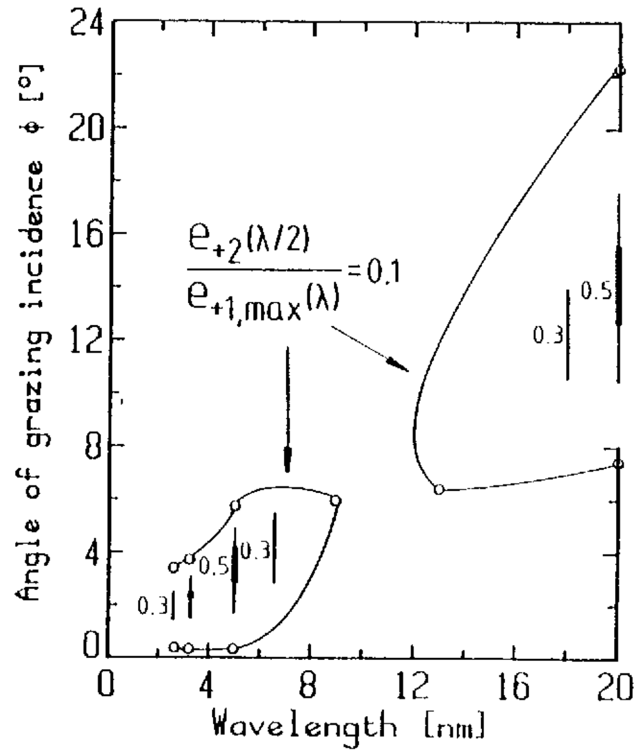
Angle of grazing incidence Φ [°]
Wavelength [nm]
0
4
8
12
16
20
24
$\frac{e_{+2}(\lambda/2)}{e_{+1,max}(\lambda)} = 0.1$
0.3
0.5

Fig 9